Published in final edited form as:
Mol Cell Proteomics. 2005 September ; 4(9): 1350–1357.

Analysis of Intimal Proteoglycans in Atherosclerosis-prone and Atherosclerosis-resistant Human Arteries by Mass Spectrometry[*,S]

Paul Talusan[‡,¶], **Shahinaz Bedri**[‡], **Suping Yang**[‡], **Taj Kattapuram**[‡], **Nilsa Silva**[‡], **Peter J. Roughley**[¶], and **James R. Stone**[‡,‖]

‡ *From the Department of Pathology, Massachusetts General Hospital, Harvard Medical School, Boston, Massachusetts 02114,*

¶ *Division of Graduate Medical Sciences, Boston University School of Medicine, Boston, Massachusetts 02118,* ¶*Genetics Unit, Shriners Hospital for Children, and Department for Surgical Research, Department of Surgery, McGill University, Montreal, Quebec H3G 1A6, Canada*

Abstract

The propensity to develop atherosclerosis varies markedly among different sites in the human vasculature. To determine a possible cause for such differences in atherosclerosis susceptibility, a proteomics-based approach was used to assess the extracellular proteoglycan core protein composition of intimal hyperplasia from both the atherosclerosis-prone internal carotid artery and the atherosclerosis-resistant internal thoracic artery. The intimal proteoglycan composition in these preatherosclerotic lesions was found to be more complex than previously appreciated with up to eight distinct core proteins present, including the large extracellular proteoglycans versican and aggrecan, the basement membrane proteoglycan perlecan, the class I small leucine-rich proteoglycans biglycan and decorin, and the class II small leucine-rich proteoglycans lumican, fibromodulin, and prolargin/PRELP (proline arginine-rich end leucine-rich repeat protein). Although most of these proteoglycans seem to be present in similar amounts at the two locations, there was a selective enhanced deposition of lumican in the intima of the atherosclerosis-prone internal carotid artery compared with the intima of the atherosclerosis-resistant internal thoracic artery. The enhanced deposition of lumican in the intima of an atherosclerosis prone artery has important implications for the pathogenesis of atherosclerosis.

An important unexplained observation concerning atherosclerosis is the marked variability in susceptibility of different sites in the human vasculature to the development of the disease. For example, whereas the internal carotid and coronary arteries show marked susceptibility to the development of atherosclerosis, the internal thoracic and distal ulnar arteries are markedly resistant to it, despite routinely forming intimal hyperplasia (1–5). In humans, atherosclerotic lesions develop at sites of intimal hyperplasia or intimal thickening, and such lesions are regarded as precursor lesions for atherosclerosis (6,7). Altered shear stresses distal to vascular branch points are likely to be responsible for the formation of much of the intimal hyperplasia in the human vasculature, and such altered shear forces are a plausible explanation for the characteristic eccentric appearance of intimal hyperplasia at these sites (8–10). However, there is currently no sufficient explanation for why such intimal hyperplasia will routinely progress to atherosclerosis at some locations, but not others, in the vasculature.

[*]This work was supported by National Institutes of Health Grant HL074324.

[S]The online version of this article (available at http://www.mcponline.org) contains supplemental material.

‖ To whom correspondence should be addressed: Dept. of Pathology, Warren 501B, Massachusetts General Hospital, 55 Fruit St., Boston, MA 02114. Tel.: 617-726-8303; Fax: 617-726-2365; E-mail jrstone@partners.org..

Intimal proteoglycans are up-regulated at sites of intimal hyperplasia and seem to play a direct role in the development of atherosclerosis by binding and retaining apolipoprotein-B containing lipoproteins in the vessel wall and by regulating vascular cell growth (11–15). The lipoproteins sequestered in the intima probably stimulate a chronic inflammatory response, resulting in the accumulation of macrophages and the development of a necrotic/lipid core (16–18). Because proteoglycans deposited in intimal hyperplasia are believed to play a central role in the development of atherosclerosis, it was hypothesized that differences in the intimal extracellular proteoglycan composition may be at least partly responsible for the marked variation in susceptibility to atherosclerosis among different sites in the vasculature.

Our previous understanding of the extracellular proteoglycan composition of human vascular intima has been relatively limited. Biglycan was definitively demonstrated in human intima by protein sequencing (19). In addition, immunologic and/or mRNA transcript analyses have provided evidence for additional proteoglycans in human intima, predominantly versican, decorin, perlecan, and lumican (20–26). It is noteworthy that these immunohistochemical analyses have indicated that versican, biglycan, and lumican are present in both atherosclerotic lesions and preatherosclerotic intimal hyperplasia. In contrast, immunoreactivity for decorin has been reported to be present in atherosclerotic lesions but absent in intimal hyperplasia (20).

To gain a more complete understanding of the extracellular proteoglycan core protein composition of human vascular intima and how this composition may vary at different sites in the circulation, a proteomics-based approach was performed using both the atherosclerosis-prone internal carotid artery and the atherosclerosis-resistant internal thoracic artery. This analysis revealed that the extracellular proteoglycan core protein composition of human intimal hyperplasia is substantially more complex than previously realized. Furthermore, these studies have revealed that there is enhanced deposition of the class II small leucine-rich proteoglycan lumican in the intima of the atherosclerosis-prone internal carotid artery.

EXPERIMENTAL PROCEDURES

Arterial Specimens

Arterial segments were obtained from autopsies performed at Massachusetts General Hospital within 24 h of death from patients ranging in age from the 4th to 10th decades of life. Cases were excluded if there was a history of prior surgery or radiation therapy involving the arterial segments. The Hospital's Human Subjects Institutional Review Board approved all activities. The left internal carotid artery at the level of the carotid bifurcation and the internal thoracic arteries at the level of the bifurcation of the intercostal arteries below the second rib were carefully identified and removed. A representative cross-section was fixed in 10% buffered formalin for 16 h, processed with paraffin embedding, and used to generate hematoxylin-and-eosin-stained histological slides. The remainder of the tissue was stored at −80 °C for proteomic analysis. For this study, an atherosclerotic lesion was defined as the presence of numerous foam cells or a necrotic/lipid core, which included classic type II lesions and above (27). For this study, intimal hyperplasia was defined as an intima greater than 0.03 mm thick with or without isolated/focal foam cells. Vessels with an intimal thickness of less than 0.03 mm were considered normal. Morphometric analyses were performed using a Nikon Eclipse E600 microscope equipped with a Hitachi HV-C20 3-CCD digital camera with computer interface and IPLab Spectrum software (Signal Analytics, Vienna, VA). Immunohistochemical analyses for the macrophage marker CD68 and for aggrecan were performed using the VECTASTAIN Elite peroxidase-conjugated avidin-biotin method (Vector Laboratories) after antigen retrieval with Borg decloaker solution (Biocare Medical). Monoclonal anti-CD68 antibody (DakoCytomation) was used at 1:800 dilution, and goat polyclonal anti-aggrecan antibody (Santa Cruz Biotechnology) was used at 1:100 dilution. Macrophages were identified as cells

staining positively for CD68. The number of macrophages present in an arterial section was then determined by visual inspection with a microscope and manual counting. The number of macrophages present was then divided by the intimal area (in square millimeters) determined by morphometric analysis.

Proteoglycan Extraction

Arteries were rinsed in cold phosphate-buffered saline (67 mM phosphate and 150 mM NaCl, pH 7.0) and opened longitudinally. The thickened intima was carefully removed and finely diced with a razor blade. The accuracy of the intimal dissection was verified by histological analysis. To account for the larger size of the internal carotid arteries, both segments of internal thoracic artery from a given patient were processed together. The intimal tissue fragments were extracted with 8 ml of buffer A (50 mM Tris, pH 7.4, containing 7 M urea, 0.1 M NaCl, complete protease inhibitor mixture (Roche Applied Science; 1 tablet/50 ml), and 5 mM dithiothreitol) for 48 h at 4 °C. Afterward, the samples were centrifuged at 3000 × *g* for 5 min to remove the tissue fragments. Aliquots (0.1 ml) of the supernatant were retained for total protein determination, using the Bradford microassay (Bio-Rad).

To the remaining supernatant was added 50 μl of hydrated Macro-Prep High Q Support strong anion exchange resin (Bio-Rad). The mixture was incubated at 4 °C with rocking for 20 min. The resin and bound proteoglycans were sedimented by centrifugation for 5 min at 3000 × *g*. The resin was placed in a spin column and washed sequentially with the following buffers by application of 0.5 ml of the buffer followed by centrifugation for 5 min at 3000 × *g*: 1 wash with buffer A, followed by 2 washes with buffer B (buffer A with an additional 0.1 M NaCl), followed by three washes with buffer C (6 M urea, 0.2 M NaCl, and 50 mM sodium acetate, pH 3.7), and finally two washes with buffer B. The proteoglycans were then eluted from the resin by the application of 100 μl of 50 mM Tris, pH 7.4, containing 6 M urea and 1 M NaCl, followed by centrifugation for 5 min at 3000 × *g*. Aliquots of the purified proteoglycans were electrophoresed into a short (1 cm) 4% SDS-PAGE gel, which was subsequently fixed with 40% methanol, 10% acetic acid, and then stained with colloidal Coomassie (Bio-Rad).

Mass Spectrometry

Gel portions containing the proteoglycans were subjected to tryptic in-gel digestion and the tryptic peptides were extracted and separated by nanoscale reverse-phase high performance liquid chromatography followed by electrospray ionization as described in detail previously (28). Tandem mass spectra were obtained on a Finnigan LTQ linear ion-trap mass spectrometer (Thermo Electron Corporation) in the Taplin Biological Mass Spectrometry Facility in the Department of Cell Biology at Harvard Medical School. Every MS/MS spectrum obtained was used to search the human NCI database (130,741 protein entries when searched) using Sequest version 27.9. The database was searched using no enzyme specificity and a precursor ion mass accuracy of ±1 Da, allowing for the differential modification of Met (+16 Da, oxidation) and Cys (+71 Da, monoacrylamide) and for up to three missed cleavages sites. After the initial search, non-tryptic peptide matches were discarded. The remaining matches were manually inspected for quality. Those matches typically considered true matches had dCn scores of at least 0.1 and XCorr values of 2.0 or greater for +1 and +2 charged peptides and 3.5 or greater for +3 charged peptides. A particular proteoglycan was considered to be present only if 2 or more such high quality peptides were identified in at least one of the intimal preparations.

Initial preliminary assessments of the relative quantities of the various proteoglycans were based on the MS intensities of specific peptides observed in most/all of the samples. These peptides were as follows: versican (LLASDAGLYR, LATVGELQAAWR, and ETTVLVAQNGNIK), biglycan (LGLGHNQIR), decorin (SSGIENGAFQGMK), perlecan (SIEYSPQLEDAGSR and LEGDTLIIPR), lumican (SLEDLQLTHNK and

LKEDAVSAAFK), and fibromodulin (IPPVNTNLENLYLQGNR and YLPFVPSR). In cases in which more than one commonly occurring peptide was used for a particular proteoglycan, the signal intensities for the peptides were averaged. To compensate for the variation in the amount of intimal tissue removed from the different arterial segments, all MS intensity values were normalized to the total amount of protein extracted from the intimal portions. Statistical analyses (Student's *t* tests) were performed using GraphPad software.

Immunoblotting

Aliquots of the purified proteoglycans were subjected to SDS-PAGE on 4–20% gradient polyacrylamide gels (Bio-Rad) and electrophoresed at 200 volts. Gels were blotted onto PVDF membrane. Membranes were probed with primary antibodies to fibromodulin (1:200 dilution), biglycan (1:1000 dilution), or lumican (1:1000 dilution). Goat polyclonal antibodies to fibromodulin were obtained from Santa Cruz Biotechnology. Rabbit polyclonal antibodies to lumican and biglycan were prepared as described previously (29,30). Blots were then treated with the appropriate peroxidase-conjugated secondary antibody: donkey anti-goat (Jackson) at 1:5000 dilution or donkey anti-rabbit (Santa Cruz) at 1:2000 dilution. Blots were imaged using ECL-plus chemiluminescence detection kits (Amersham Biosciences) and film which was developed on an X-Omat processor. Bands were quantitated using a GS-800 laser densitometer (Bio-Rad). To compensate for the variation in the amount of intimal tissue removed from the different arterial segments, all chemiluminescence values were normalized to the total amount of protein extracted from the intimal portions. Statistical analyses (Student's *t* tests) were performed using GraphPad software.

RESULTS

Arterial Specimens

Left internal carotid arteries at the level of the carotid bifurcation and/or internal thoracic arteries at the level of the bifurcation of the intercostal arteries below the second rib were obtained from 56 randomly selected autopsies. Both of these arterial segments are elastic arteries (in contrast to muscular arteries) and are thus amenable to direct comparison for differences in extracellular matrix composition. Histological analysis revealed 27 of 45 left internal carotid arteries to have developed atherosclerotic lesions, with 16 of the remaining 18 cases showing intimal hyperplasia. In contrast, atherosclerosis was present in the internal thoracic arteries from only 7 of 53 patients, confirming the atherosclerosis resistance of this site ($p < 0.0001$; Fig. 1). It is noteworthy that of the 46 patients without atherosclerosis in the internal thoracic arteries, 16 had developed significant eccentric intimal hyperplasia, most likely secondary to non-laminar shear forces at this postbifurcation site (8–10). Thus, like the distal ulnar artery (4), the internal thoracic artery routinely develops intimal hyperplasia yet remains relatively resistant to the formation of atherosclerosis.

The extracellular proteoglycan composition of the intimal hyperplasia from these 16 left internal carotid arteries was compared with that of the intimal hyperplasia from the 16 pairs of internal thoracic arteries. The specifics of these 32 cases are listed in Table I. There was no significant difference between these two groups of vessels with regard to patient age, gender, or macrophage density. Likewise, although there was a slight trend toward increasing frequency of isolated/focal foam cells in the carotid artery segments, this difference was not statistically significant. There was an enhanced ratio of intimal-to-medial thickness in the internal carotid arteries compared with the internal thoracic arteries. Overall, these two groups of arterial segments were very well matched for histologic lesion type, with both displaying preatheromatous intimal hyperplasia. These two groups of vessels were used to compare the intimal proteoglycan composition of the preatherosclerotic lesions at these two distinct sites, which differ markedly in their propensity to develop atherosclerosis.

Intimal Proteoglycan Composition

For each arterial segment, the thickened intima was carefully removed (Fig. 2), and the proteoglycans were extracted and analyzed by liquid chromatography tandem mass spectrometry (Table II; Fig. 3). Consistent with previous immunohistochemistry studies (20–23,25,26), versican, biglycan, and perlecan were detected in the intimal extracts from nearly all of the vessels examined. The greatest numbers of peptides were routinely observed for these three proteoglycans, consistent with the notion that they represent the major proteoglycans in intimal hyperplasia. Immunoreactivity corresponding to the class II SRL proteoglycan lumican has been observed in both atherosclerotic lesions and intimal hyperplasia (24). Consistent with these findings, by mass spectrometry lumican was detected in intimal hyperplasia in most of the specimens analyzed here. In contrast to previous immunohistochemical studies (20), decorin was also routinely observed in these preatherosclerotic lesions, probably because of the enhanced sensitivity of this mass spectrometry-based approach. In addition to these previously recognized components of human intima, proteoglycans not previously known to occur in human intimal hyperplasia were observed. There were the large extracellular proteoglycan aggrecan and the class II small leucine-rich proteoglycans fibromodulin and prolargin/PRELP (proline arginine-rich end leucine-rich repeat protein). Thus, overall, the extracellular proteoglycan composition of human intimal hyperplasia was found to be significantly more complex than previously realized, with up to eight distinct core proteins present in these preatherosclerotic lesions.

MS Signal Intensities

As an initial assessment for large variations in the quantities of these proteoglycans, MS intensities for peptides from the more frequently occurring proteoglycans were compared. Although there was a slight trend toward increasing signal intensities for versican, biglycan, and fibromodulin in the internal carotid arteries, the differences were not statistically significant (Fig. 4). This was also the case for perlecan and decorin (data not shown). However, there was a statistically significant ($p < 0.01$) enhancement in the signal intensities for lumican in the atherosclerosis-prone internal carotid artery compared with those from the atherosclerosis-resistant internal thoracic artery.

Immunoblotting

To confirm the enhanced deposition of lumican in the atherosclerosis-prone artery, immunoblotting for selected proteoglycans was performed on these samples (Fig. 5). By immunoblot analysis, biglycan is present as two distinct forms with apparent masses of ~100 and ~250 kDa (Fig. 5*A*). These two forms of biglycan have been observed previously in tissues and cultured vascular cells (31,32). However, the structural feature that gives rise to these two forms of biglycan is not known. Quantitation of the total biglycan present by immunoblotting revealed no significant difference between the atherosclerosis-prone and atherosclerosis-resistant arteries, consistent with the analysis of MS signal intensities. In addition, there was no significant difference in the relative amounts of the two forms of biglycan between the two arterial locations (data not shown). By immunoblotting, fibromodulin is present as both a sharp band with an apparent mass of ~50 kDa and a more diffuse band with an apparent mass of ~80 kDa (Fig. 5*B*). The lower band may represent a tyrosine sulfated core protein lacking carbohydrate modification, and the upper band probably represents a form with carbohydrate modifications (33). Again, consistent with the analyses of the MS signal intensities, there was no difference in the amount of fibromodulin present in intima from the two arterial locations. Immunoblotting for lumican (Fig. 5*C*) revealed multiple diffuse bands predominantly from 50–100 kDa, indicative of a proteoglycan form of lumican (33–36). Consistent with the analysis of the MS signal intensities, there was significantly ($p < 0.01$) more lumican present in the intima of the atherosclerosis-prone internal carotid artery than in the atherosclerosis-resistant

internal thoracic artery, with the mean value elevated by ~3-fold. In neither vessel did the quantity of lumican present in these early lesions correlate with age, gender, intima/media ratio, macrophage density, or the presence of focal foam cells (data not shown).

Aggrecan Immunohistochemistry

The identification of aggrecan in human intimal hyperplasia is a novel finding with important implications for vascular disease. To verify the location of aggrecan in human intima, immunohistochemistry for aggrecan was performed. Immunoreactivity for aggrecan was observed predominantly in the inner zone of intimal hyperplasia, with only very faint immunoreactivity in the deeper intima and media (Fig. 6). The inner (subendothelial) zone of intimal hyperplasia is known to be particularly rich in proteoglycans (7). The results presented here indicate that in addition to versican, aggrecan is a large extracellular proteoglycan contributing to the structure of the matrix in the proteoglycan-rich zone of the inner intima.

DISCUSSION

Previous studies, primarily employing immunohistochemistry and transcript analyses, have suggested that versican, perlecan, and biglycan are the predominant proteoglycans in human intimal hyperplasia (19–23,25–26). The mass spectrometry-based analysis reported here confirms that versican, biglycan, and perlecan are major components of the intimal extracellular matrix, with substantial protein sequence verified for each of these proteoglycans. However, this analysis also revealed that the proteoglycan core protein composition of human intimal hyperplasia is more complex than previously appreciated, containing core proteins not previously known to occur in these lesions. The roles of many of these proteoglycans in the intima remain to be elucidated. Aggrecan is of particular interest because of its large size and numerous potential glycosaminoglycan modification sites. One potential mechanism by which proteoglycans may promote atherosclerosis is by the direct binding of lipoproteins to the negatively charged glycosaminoglycan side chains (11–14). Because of the large size of aggrecan, and the large number of glycosaminoglycan modification sites, aggrecan has the potential to have the greatest affinity for lipoproteins of all of the intimal proteoglycans.

Both versican and biglycan have been implicated as playing important roles in the formation of atherosclerosis (15,23). The finding of no substantial differences in the apparent quantities of these two proteoglycans upon comparing atherosclerosis-prone and atherosclerosis-resistant arteries was unexpected. These studies cannot exclude more subtle (2-fold or less) changes in protein levels, variations in splice forms, or alterations of glycosaminoglycan side chains, which may differ between the two sites. For a given proteoglycan, there was substantial variation from case to case in the amounts detected, and the use of cadaveric material may have contributed to this variation; however, no substantial protein degradation was detected in these samples (Fig. 5). The data presented here do indicate that a major difference in the intimal hyperplasia of atherosclerosis-prone arteries compared with that in atherosclerosis-resistant arteries is the enhanced deposition of lumican in the intima of the atherosclerosis-prone arteries.

Lumican has been shown to play an important role in wound healing and tissue responses to injury, and this proteoglycan is a positive regulator of Fas-Fas ligand-mediated apoptosis (37–40). In addition, lumican has been shown to directly bind to macrophages and to enhance macrophage migration (41). These prior studies imply that lumican could directly influence macrophage behavior in the vascular intima as well as stimulate the formation of the necrotic/lipid core characteristic of advanced atherosclerotic lesions. The data presented here demonstrate that well before atheroma formation there is a significant difference in the composition of the intimal extracellular matrix of atherosclerosis-prone arteries compared with atherosclerosis-resistant arteries. Before the formation of a necrotic/lipid core, there seems to be deposited in the intima of the atherosclerosis-prone vessels an extracellular matrix with the

potential to promote inflammation and cell death. The underlying factors stimulating the formation of this atherosclerosis-prone matrix are unclear, but such factors are likely to play a central role in atherosclerotic lesion development.

Supplementary Material

Refer to Web version on PubMed Central for supplementary material.

Acknowledgements

We thank the Taplin Biological Mass Spectrometry Facility in the Department of Cell Biology at Harvard Medical School under the direction of Dr. Steven Gygi for acquisition of LC-MS/MS spectra.

References

1. Vink A, Schoneveld AH, Poppen M, de Kleijn DPV, Borst C, Pasterkamp G. Morphometric and immunohistochemical characterization of the intimal layer throughout the arterial system of elderly humans. J Anat 2002;200:97–103. [PubMed: 11837253]
2. Ruengsakulrach P, Sinclair R, Komeda M, Raman J, Gordon I, Buxton B. Comparative histopathology of radial artery versus internal thoracic artery and risk factors for development of intimal hyperplasia and atherosclerosis. Circulation 1999;100:II–139–II–144.
3. Fishbein MC, Hartman G. Pathology of internal mammary arteries used as bypass grafts. Cardiovasc Pathol 1997;6:31–33.
4. Stone JR. Intimal hyperplasia in the distal ulnar artery: influence of gender and implications for the hypothenar hammer syndrome. Cardiovasc Pathol 2004;13:20–25. [PubMed: 14761781]
5. Wright I. The microscopical appearances of human peripheral arteries during growth and aging. J Clin Pathol 1963;16:499–522. [PubMed: 14076367]
6. Schwartz SM, deBlois D, O'Brien ERM. The intima: soil for atherosclerosis and restenosis. Circ Res 1995;77:445–465. [PubMed: 7641318]
7. Stary HC, Blankenhorn DH, Chandler AB, Glagov S, Insull W, Richardson M, Rosenfeld ME, Schaffer SA, Schwartz CJ, Wagner WD, Wissler RW. A definition of the intima of human arteries and of its atherosclerosis-prone regions. Circulation 1992;85:391–405. [PubMed: 1728483]
8. Davies PF. Flow-mediated endothelial mechanotransduction. Physiol Rev 1995;75:519–560. [PubMed: 7624393]
9. Garcia-Cardena G, Comander J, Anderson KR, Blackman BR, Gimbrone MA. Biomechanical activation of vascular endothelium as a determinant of its functional phenotype. Proc Natl Acad Sci U S A 2001;98:4478–4485. [PubMed: 11296290]
10. Traub O, Berk BC. Laminar shear stress: Mechanisms by which endothelial cells transduce an atheroprotective force. Arterioscler Thromb Vasc Biol 1998;18:677–685. [PubMed: 9598824]
11. Skålén K, Gustafsson M, Rydberg EK, Hultén LM, Wiklund O, Innerarity TL, Borén J. Subendothelial retention of atherogenic lipoproteins in early atherosclerosis. Nature 2002;417:750–754. [PubMed: 12066187]
12. Williams KJ. Arterial wall chondroitin sulfate proteoglycans: diverse molecules with distinct roles in lipoprotein retention and atherogenesis. Curr Opin Lipidol 2001;12:477–487. [PubMed: 11561166]
13. Camejo G, Hurt-Camejo E, Wiklund O, Bondjers G. Association of apo B lipoproteins with arterial proteoglycans: pathological significance and molecular basis. Atherosclerosis 1998;139:205–222. [PubMed: 9712326]
14. Williams KJ, Tabas I. The response-to-retention hypothesis of early atherogenesis. Arterioscler Thromb Vasc Biol 1995;15:551–561. [PubMed: 7749869]
15. Wight TN, Merrilees MJ. Proteoglycans in atherosclerosis and restenosis, key roles for versican. Circ Res 2004;94:1158–1167. [PubMed: 15142969]
16. Becker AE, de Boer OJ, van der Wal AC. The role of inflammation and infection in coronary artery disease. Annu Rev Med 2001;52:289–297. [PubMed: 11160780]
17. Libby P. Inflammation in atherosclerosis. Nature 2002;420:868–874. [PubMed: 12490960]

18. Glass CK, Witztum JL. Atherosclerosis: the road ahead. Cell 2001;104:503–516. [PubMed: 11239408]
19. Stöcker G, Meyer HE, Wagener C, Greiling H. Purification and *N*-terminal amino acid sequence of a chondroitin sulphate/dermatan sulphate proteoglycan isolated from intima/media preparations of human aorta. Biochem J 1991;274:415–420. [PubMed: 1848758]
20. Gutierrez P, O'Brien KD, Ferguson M, Nikkari ST, Alpers CE, Wight TN. Differences in the distribution of versican, decorin, and biglycan in atherosclerotic human coronary arteries. Cardiovasc Pathol 1997;6:271–278.
21. Kolodgie FD, Burke AP, Farb A, Weber DK, Kutys R, Wight TN, Virmani R. Differential accumulation of proteoglycans and hyaluronan in culprit lesions: insights into plaque erosion. Arterioscler Thromb Vasc Biol 2002;22:1642–1648. [PubMed: 12377743]
22. Lin H, Kanda T, Hoshino Y, Takase SI, Kobayashi I, Nagai R, McManus BM. Versican, biglycan, and decorin protein expression patterns in coronary arteries: analysis of primary and restenotic lesions. Cardiovasc Pathol 1998;7:31–37.
23. O'Brien KD, Olin KL, Alpers CE, Chiu W, Ferguson M, Hudkins K, Wight TN, Chait A. Comparison of apolipoprotein and proteoglycan deposits in human coronary atherosclerotic plaques: co-localization of biglycan with apolipoproteins. Circulation 1998;98:519–527. [PubMed: 9714108]
24. Onda M, Ishiwata T, Kawahara K, Wang R, Naito Z, Sugisaki Y. Expression of lumican in thickened intima and smooth muscle cells in human coronary atherosclerosis. Exp Mol Pathol 2002;72:142–149. [PubMed: 11890723]
25. Chung IM, Gold HK, Schwartz SM, Ikari Y, Reidy MA, Wight TN. Enhanced extracellular matrix accumulation in restenosis of coronary arteries after stent deployment. J Am Col Cardiol 2002;40:2072–2081.
26. Murdoch AD, Iozzo RV. Perlecan: the multidomain heparan sulphate proteoglycan of basement membrane and extracellular matrix. Virchows Archiv A Pathol Anat 1993;423:237–242.
27. Stary HC, Chandler AB, Glagov S, Guyton JR, Insull W, Rosen-feld ME, Schaffer SA, Schwartz CJ, Wagner WD, Wissler RW. A definition of initial, fatty streak, and intermediate lesions of atherosclerosis. Circulation 1994;89:2462–2478. [PubMed: 8181179]
28. Stone JR, Maki JL, Collins T. Basal and hydrogen peroxide stimulated sites of phosphorylation in heterogeneous nuclear ribonucleoprotein C1/C2. Biochemistry 2003;42:1301–1308. [PubMed: 12564933]
29. Grover J, Chen XN, Korenberg JR, Roughley PJ. The human lumican gene: organization, chromosomal location, and expression in articular cartilage. J Biol Chem 1995;270:21942–21949. [PubMed: 7665616]
30. Roughley PJ, White RJ, Mort JS. Presence of pro-forms of decorin and biglycan in human articular cartilage. Biochem J 1996;318:779–784. [PubMed: 8836119]
31. Plaas AHK, Wong-Palms S, Koob T, Hernandez D, Marchuk L, Frank CB. Proteoglycan metabolism during repair of the ruptured medial collateral ligament in skeletally mature rabbits. Arch Biochem Biophys 2000;374:35–41. [PubMed: 10640393]
32. Jarvelainen HT, Kinsella MG, Wight TN, Sandell LJ. Differential expression of small chondroitin/dermatan sulfate proteoglycans, PG-I/biglycan and PG-II/decorin, by vascular smooth muscle and endothelial cells in culture. J Biol Chem 1991;266:23274–23281. [PubMed: 1744124]
33. Sztrolovics R, Alini M, Mort JS, Roughley PJ. Age-related changes in fibromodulin and lumican in human intervertebral discs. Spine 1999;24:1765–1771. [PubMed: 10488504]
34. Funderburgh JL, Funderburgh ML, Mann MM, Conrad GW. Arterial lumican: properties of a corneal-type keratan sulfate proteoglycan from bovine aorta. J Biol Chem 1991;266:24773–24777. [PubMed: 1761572]
35. Dolhnikoff M, Morin J, Roughley PJ, Ludwig MS. Expression of lumican in human lungs. Am J Respir Cell Mol Biol 1998;19:582–587. [PubMed: 9761754]
36. Qin H, Ishiwata T, Asano G. Effects of the extracellular matrix on lumican expression in rat aortic smooth muscle cells in vitro. J Pathol 2001;195:604–608. [PubMed: 11745697]
37. Saika S, Shiraishi A, Saika S, Liu CY, Funderburgh JL, Kao CWC, Converse RL, Kao WWY. Role of lumican in the corneal epithelium during wound healing. J Biol Chem 2000;275:2607–2612. [PubMed: 10644720]

38. Yeh LK, Chen WL, Li W, Espana EM, Ouyang J, Kawakita T, Kao WWY, Tseng SCG, Liu CY. Soluble lumican glycoprotein purified from human amniotic membrane promotes corneal epithelial wound healing. Investig Ophthalmol Vis Sci 2005;46:479–486. [PubMed: 15671272]

39. Vij N, Roberts L, Joyce S, Chakravarti S. Lumican regulates corneal inflammatory responses by modulating Fas-Fas ligand signaling. Investig Ophthalmol Vis Sci 2005;46:88–95. [PubMed: 15623759]

40. Vij N, Roberts L, Joyce S, Chakravarti S. Lumican suppresses cell proliferation and aids Fas-Fas ligand mediated apoptosis: implications in the cornea. Exp Eye Res 2004;78:957–971. [PubMed: 15051477]

41. Funderburgh JL, Mitschler RR, Funderburgh ML, Roth MR, Chapes SK, Conrad GW. Macrophage receptors for lumican: a corneal keratan sulfate proteoglycan. Investig Ophthalmol Vis Sci 1997;38:1159–1167. [PubMed: 9152235]

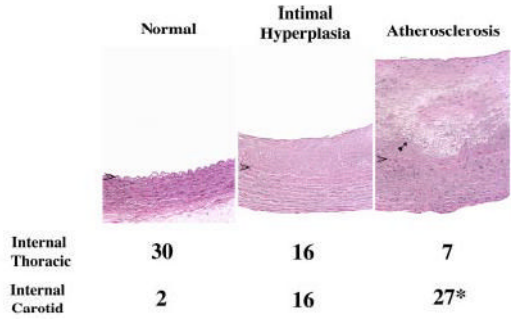

Fig. 1. Classification of vascular lesions

The arterial segments were classified as to the lesion type present based on histologic analysis, as defined under "Experimental Procedures." Shown are representative histologic images of hematoxylin-and-eosin-stained sections of internal thoracic arteries at 100× magnification. The *arrowheads* indicate the intima/media boundaries. The *arrow* indicates a developing necrotic/lipid core. The *numbers* indicate the number of cases for each vessel with the corresponding lesion type, demonstrating the marked difference in atherosclerosis susceptibility of these two arteries. *, $p < 0.0001$.

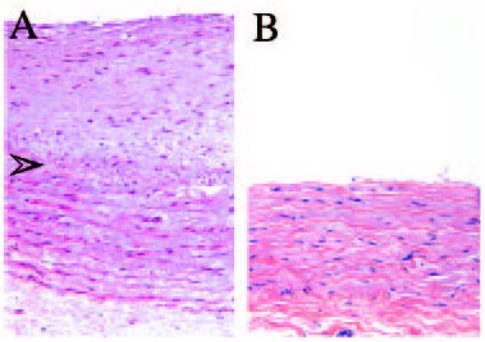

Fig. 2. Removal of thickened intima for proteomic analysis

Shown is a representative section of an internal thoracic artery stained with hematoxylin and eosin at 200× magnification before (*A*) and after (*B*) removal of the thickened intima. The *arrowhead* indicates the level of the intima/media boundary.

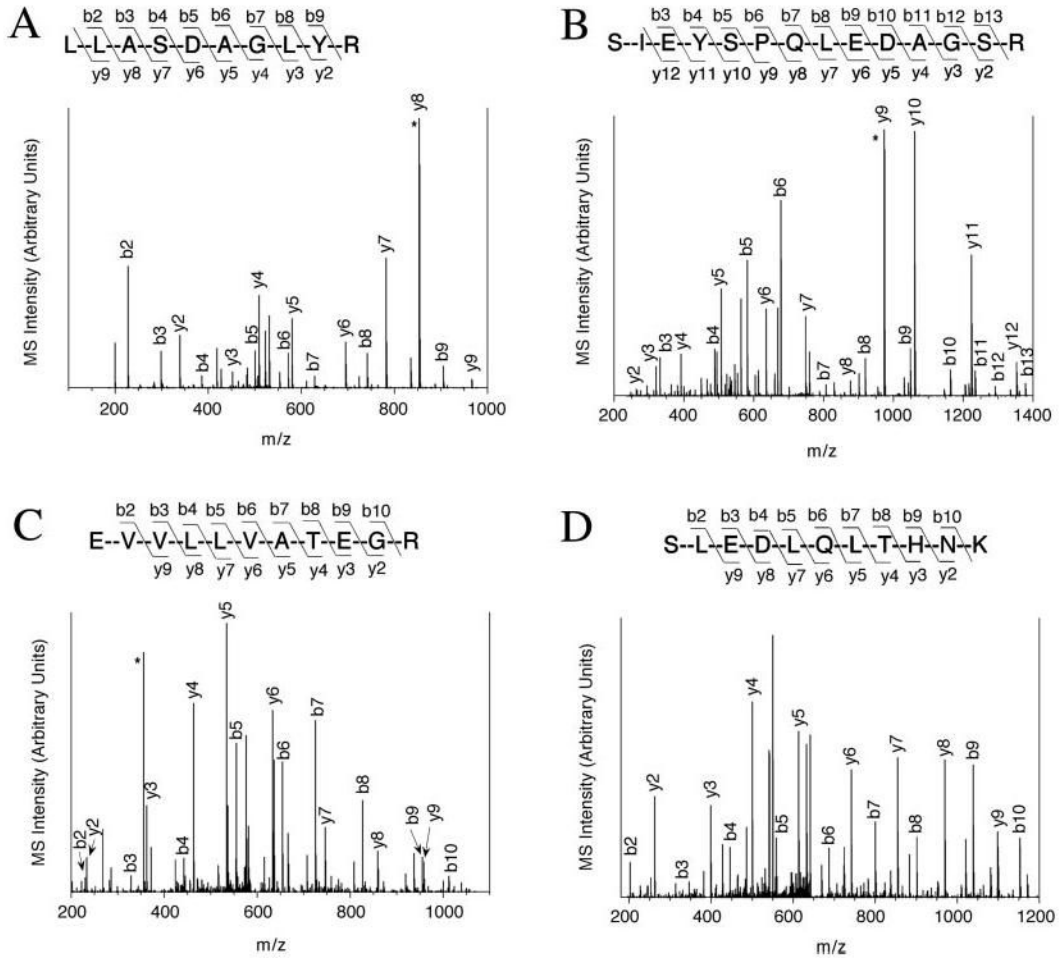

Fig. 3. Proteoglycans in human vascular intima

Representative tandem mass spectra showing the identification of versican (*A*), perlecan (*B*), aggrecan (*C*), and lumican (*D*). Some peaks (*) have been scaled by 50% for presentation.

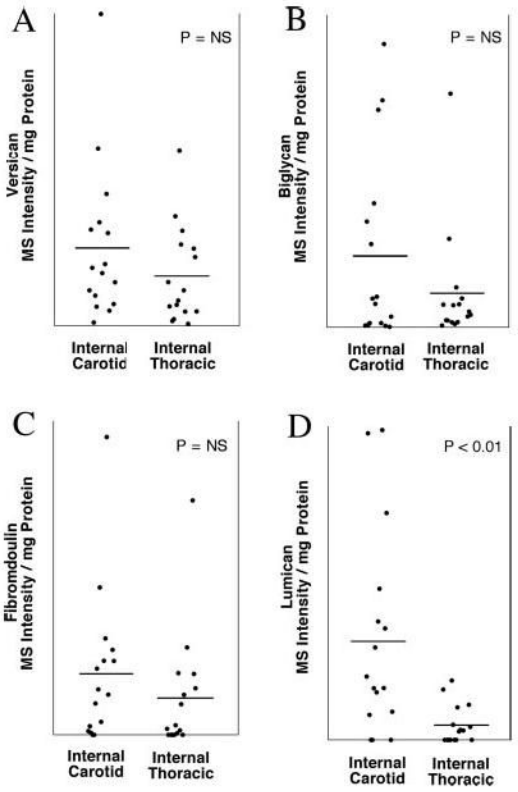

Fig. 4. Enhanced MS signal intensity for lumican in the atherosclerosis-prone internal carotid artery

MS signal intensities for selected peptides from versican (*A*), biglycan (*B*), fibromodulin (*C*), and lumican (*D*) from the two arterial sites were compared. *Horizontal bars* indicate the mean values.

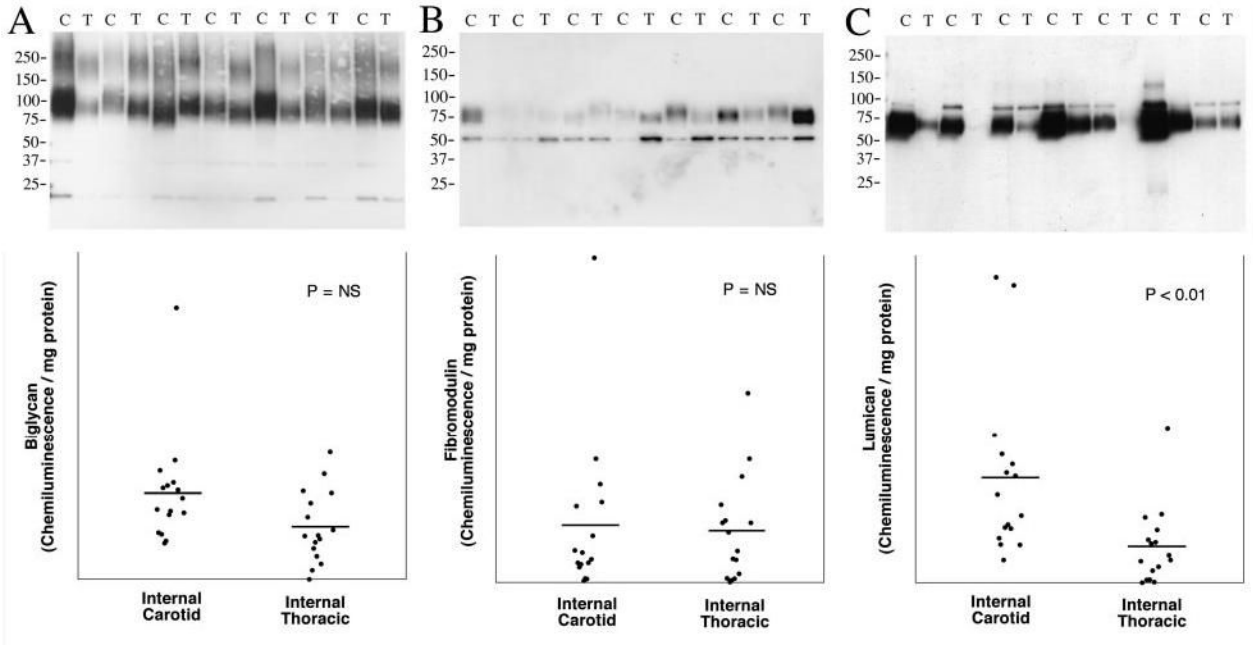

Fig. 5. Lumican is up-regulated in the atherosclerosis-prone internal carotid artery

Shown are representative immunoblots (*top*) for biglycan (*A*), fibromodulin (*B*), and lumican (*C*), with alternating internal carotid "C" and internal thoracic "T" arteries. The *scales to the left* indicate the molecular mass markers in kilodaltons. The *bottom* depicts the quantitation of the chemiluminescence signals. The *horizontal bars* indicate the mean values. *NS*, not significant.

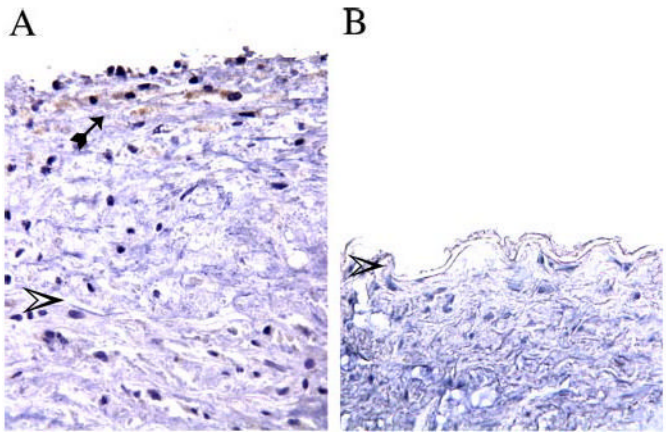

Fig. 6. Aggrecan is an intimal proteoglycan

A, immunohisto-chemical stain for aggrecan in an internal carotid artery with intimal hyperplasia (400× magnification) showing aggrecan immunoreactivity in the inner intima (*arrow*). *B*, immunohistochemical stain for aggrecan in a normal internal carotid artery lacking intimal hyperplasia (400× magnification) demonstrating no significant aggrecan immunoreactivity. The *arrowheads* indicate the intima/media boundaries.

Table I

Characteristics of the arteries used for determination of intimal proteoglycans

Vessel	Internal carotid	Internal thoracic
Number	16	16
Age (years)	63 ± 20	71 ± 17
Gender (M/F)	7/9	10/6
Focal foam cells (present/absent)	13/3	9/7
Macrophages/mm^2	47 ± 72	45 ± 72
Intima/media ratio	0.9 ± 0.7*	0.4 ± 0.3

* $p < 0.01$ *versus* internal thoracic artery.

Table II

Intimal proteoglycans observed in atherosclerosis-prone and atherosclerosis-resistant arteries

The complete list of all peptides identified for each proteoglycan is included in the supplemental material.

	Internal carotid			Internal thoracic		
	Frequency	No. of peptides	Sequence coverage	Frequency	No. of peptides	Sequence coverage
	%		%	%		%
Large extracellular proteoglycans						
Versican	100	4–17	1–5	100	5–11	2–4
Aggrecan	13	1–8	0.3–2	38	1–6	0.5–2
Basement membrane proteoglycans						
Perlecan	94	3–22	1–6	100	3–27	1–8
Class I SLR-proteoglycans						
Biglycan	100	5–15	16–52	100	4–15	11–51
Decorin	94	1–5	4–20	88	1–7	4–22
Class II SLR-proteoglycans						
Fibromodulin	88	1–4	5–11	75	1–4	2–11
Lumican	81	1–8	3–31	56	2–6	6–25
Prolargin / PRELP	56	2–7	5–20	44	1–4	3–11